

Rovibrational spectroscopy of the CH^+ -He and CH^+ -He₄ complexes

Thomas Salomon^a, José L. Doménech^b, Philipp C. Schmid^a, Ernest A. Michael^{a,c}, Stephan Schlemmer^a, Oskar Asvany^a

^a*I. Physikalisches Institut, Universität zu Köln, Zùlpicher Str. 77, 50937 Köln, Germany*

^b*Instituto de Estructura de la Materia (IEM-CSIC), Serrano 123, 28006 Madrid, Spain*

^c*Department of Electrical Engineering, University of Chile, Av. Tupper 2007, Santiago, Chile*

Abstract

A cryogenic 22-pole ion trap apparatus is used in combination with a table-top pulsed IR source to probe weakly bound CH^+ -He and CH^+ -He₄ complexes by predissociation spectroscopy at 4 K. The infrared photodissociation spectra of the C-H stretching vibrations are recorded in the range of 2720–2800 cm^{-1} . The spectrum of CH^+ -He exhibits perpendicular transitions of a near prolate top with a band origin at 2745.9 cm^{-1} , and thus confirms it to have a T-shaped structure. For CH^+ -He₄, the C-H stretch along the symmetry axis of this oblate top results in parallel transitions.

Keywords: ion trap, rovibrational spectroscopy, CH^+ -He

1. Introduction

Molecular complexes consisting of a cation and a weakly bound neutral partner have been investigated by action spectroscopy in the last four decades. These techniques were primarily invented and used to obtain spectroscopic information about the bare cation itself [1, 2, 3, 4, 5], but more recently the focus shifted also towards the weak interaction between the constituents and the corresponding shallow potential energy surface (PES), in particular for floppy cation-helium complexes. For instance, IR spectra, and, more recently, also partly rotational spectra of N_2H^+ -He [6], HCO^+ -He [7, 8], OH^+ -He [9], CH_3^+ -He [10, 11], N_2^+ -He [12], NH_4^+ -He [13], O_2H^+ -He [14, 15], H_3^+ -He [16] and H^+ -He_n [17, 18] have been explored.

CH^+ was the very first molecular ion known to exist in interstellar space, detected by its electronic transitions [19, 20], and since then it has also been detected by its rotational [21, 22, 23, 24], and vibrational [25] transitions (the latter only very recently). In the astronomically important collision between CH^+ and He the weakly bound CH^+ -He complex is formed as an intermediate. **Up to date, the CH^+ -He complex has been investigated only theoretically, first by Hughes and Nagy-Felsobuki [26], and later by Meuwly and Wright [27].** These authors predict a T-shape structure rather than a linear one, see Fig. 1. Detailed knowledge of the CH^+ -He PES is important to be able to predict inelastic collision rates in space [28, 29]. Determination of its bound states by rotational or rovibrational spectroscopy, together with theoretical work, is a very exact way of exploring the underlying PES.

In a previous work aimed at high-resolution detection of the C-H stretching fundamental of the bare CH^+ cation [30], we serendipitously found seven Lorentzian lines which we ascribed

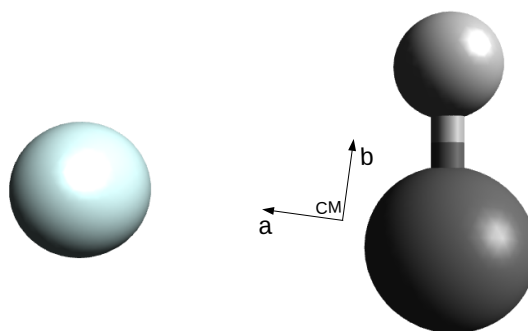


Figure 1: Sketch of CH^+ -He depicting its center of mass and its principal axes of inertia.

to CH^+ -He. In this work, we complete the search for the lines of the complex using the same ion trap machine, and apply a lower-resolution pulsed laser to record the infrared photodissociation (IRPD) spectrum of CH^+ -He. In addition, we also measure the IRPD spectrum of the symmetric complex CH^+ -He₄.

2. Experimental details

The IRPD experiments of CH^+ -He and CH^+ -He₄ are carried out in the ion trapping machine COLTRAP [31]. A 1:1 mixture of helium and methane (Linde 5.5) is used as a precursor to create CH^+ ions by electron impact ionization in an external storage ion source (electron energy about 30 eV). Helium is used in the precursor mixture because ionized helium is known to promote the fragment ion production [32]. Subsequent mass-filtering ($m = 13$ u) in a linear quadrupole ensures that a pure sample of several ten thousand CH^+ ions enters the 4 K 22-pole ion trap [33]. About 40 ms before the ion bunch reaches the trap, He buffer gas is injected into the trap via a piezo valve and is thus thermalized by collisions with the trap walls. This leads

Email address: asvany@ph1.uni-koeln.de (Oskar Asvany)

to the cooling of the incoming ions by collisions with the buffer gas. The formation of $\text{CH}^+\text{-He}$ and higher complexes $\text{CH}^+\text{-He}_n$ via ternary collision processes is promoted by the low trap temperature and the high instantaneous He number density. In the mass spectrum of Fig. 2 one can see that the complexes with $n = 1 - 4$ are readily formed, whereas complexes with $n = 5$ or even $n = 6$ have less abundance, in agreement with a shell closure at a four-membered He-ring around the CH^+ molecular axis, as suggested earlier [34].

For IRPD spectroscopy, the shown ion ensemble is trapped for a period of 2.5 s and irradiated by the pulsed infrared radiation, leading to excitation upon resonance and subsequent destruction of the complexes ($\text{CH}^+\text{-He}$ has a dissociation energy of $D_0 = 243 \text{ cm}^{-1}$ [27]). After extracting all ions from the trap, the ions are mass-filtered in the $\text{CH}^+\text{-He}$ or $\text{CH}^+\text{-He}_4$ mass channels ($m = 17$ or 29 u , see arrows in Fig. 2) by a second linear quadrupole and efficiently counted by a Daly-type detector. The predissociation spectrum is recorded by counting the number of these complexes (typical counts are on the order of 5000) as a function of the IR excitation frequency. In that way, the resonant absorption of IR photons is observed as a dip in the counts, see lower part of Fig. 3. As long-term fluctuations of the complex counts were not severe, we omitted to use a laser shutter for normalization purposes.

The pulsed IR radiation is produced by a table-top LaserVision optical parametric oscillator/amplifier (OPO/OPA) system. The OPO/OPA system is pumped with a 1064 nm Nd:YAG laser (Continuum Surelite-Ex) operating at 10 Hz and with maximum pulse energies of 600 mJ. This system has a bandwidth of 0.1 cm^{-1} when seeded. The IR laser wavelength is monitored with a wavemeter (HighFinesse WS-5) with a manufacturer-stated accuracy of 0.1 cm^{-1} . The IR beam passes through the trapping machine via two Brewster window assemblies [35] adjusted for vertical polarization and containing BaF_2 windows. Typical pulse energies are on the order of 3 mJ (in seeded mode).

3. Rovibrational spectroscopy of $\text{CH}^+\text{-He}$

During our former work [30] we serendipitously recorded seven $\text{CH}^+\text{-He}$ lines and even a single $^{13}\text{CH}^+\text{-He}$ line. The latter, at $2758.548404(5) \text{ cm}^{-1}$, is depicted in Fig. 1 of reference [30]. The seven unpublished and initially unassigned lines of $\text{CH}^+\text{-He}$ are listed in Table 1. The use of a high-resolution narrow-band cw IR source allowed to determine their positions and Voigt line profiles with high accuracy and precision (the accuracy of the used wavemeter was 30 MHz, the precision even better). Thus the lifetimes of the vibrationally excited states, in the order of 1-2 ns, could be determined (see Table 1). Two lines were recorded at even higher precision and accuracy (about 80 kHz) using a frequency comb system [36].

Similar to CH^+ ($^1\Sigma$), the complex $\text{CH}^+\text{-He}$ is a closed-shell molecule with a singlet electronic ground state. *Ab initio* calculations [26, 27] predicted its equilibrium structure to be non-linear. It has rather a T-shaped equilibrium structure with the helium atom in a distance of $R_e = 2.28 \text{ \AA}$ and angle of $\theta_e = 83^\circ$ relative to the C-H center of mass and axis, respectively (see

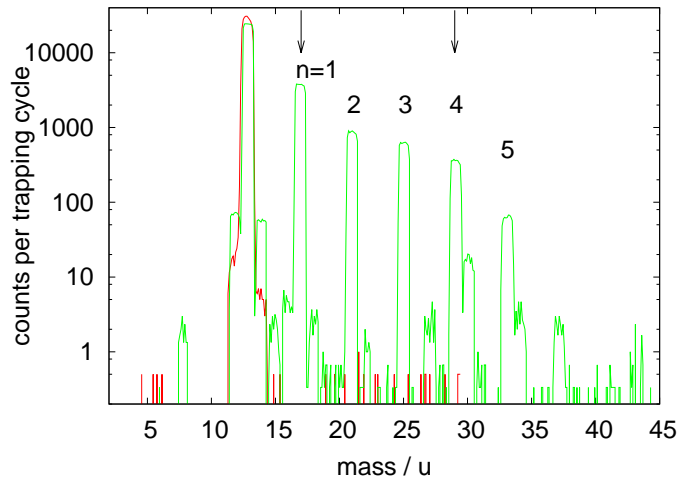


Figure 2: Mass spectra showing the trap content at time of injection (red trace) and the formation of $\text{CH}^+\text{-He}_n$ by trapping for 700 ms in a constant high-density He environment (green trace). The ion on mass 30 u is most probably due to the parasitic reaction $\text{CH}^+ + \text{H}_2\text{O} \rightarrow \text{CH}_2\text{O}^+ + \text{H}$. A similar spectrum for $\text{CD}^+\text{-He}_n$ has been given in Reference [34]. The arrows indicate the mass channels ($n = 1, 4$) in which the IRPD-detection in this work occurs.

Fig. 1). Its symmetry group is thus C_s and its ground electronic state is designated $^1A'$. Its calculated rotational constants [27] reveal that it is a near prolate top. As the C-H stretch investigated here points almost perpendicular to the symmetry axis of the prolate top (the symmetry axis is the a-axis, the C-H transition moment points almost along the b-axis), a perpendicular transition of a near prolate top can be expected.

The spectrum obtained in this work indeed resembles that of a perpendicular transition of a near prolate top. It is shown in the lower part of Fig. 3, together with the seven high-resolution lines obtained in our earlier work, depicted as blue sticks. As at least two lines of the high-resolution data set could be detected and well separated in this work, they have been used to re-calibrate the spectrum of this work (it has been shifted up by 0.13 cm^{-1} , which is well within the accuracy of the used wavemeter). The experimental spectra are accompanied by PGOPHER [37] simulations in the upper part of Fig. 3, one with narrow sticks and one convoluted with a Gaussian laser bandwidth of 0.1 cm^{-1} representative of the current experimental conditions. The fit of the simulation to the spectroscopic data yields a rotational temperature of about 10 K and spectroscopic constants as summarized in Table 2. Fortunately, we were able to resolve one asymmetry splitting in the rR_1 branch (though with low signal-to-noise ratio), which in turn enabled us to assign the formerly measured high-resolution lines with confidence, so that the parameter $B - C$ could be determined. All assigned lines are collected in Table 1. The weighted RMS of the fit is 0.29, which shows that our error limits given for the lines of this work are very conservative.

For the determination of the structure of $\text{CH}^+\text{-He}$ we assume the C-H backbone to be unchanged w.r.t. CH^+ . From the ground state rotational constant $B_{CH} = 13.9313576(1) \text{ cm}^{-1}$ [38, 30] of CH^+ we obtain a C-H bond length of $r_0 = 1.141 \text{ \AA}$. As the principal a-axis of $\text{CH}^+\text{-He}$ passes through the He atom and the center of mass of CH (see Fig. 1), the corresponding rotational

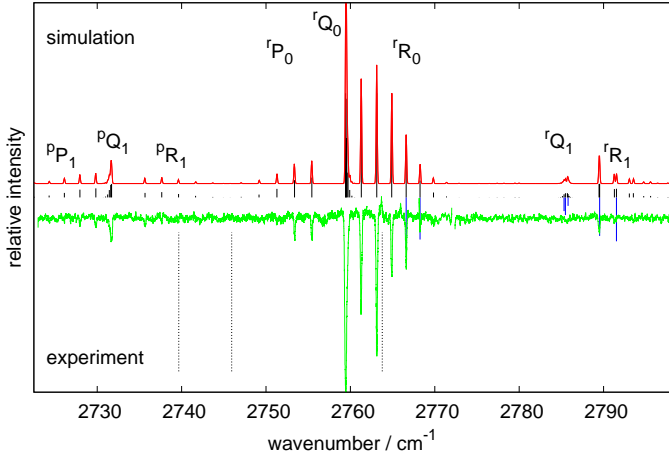


Figure 3: Rovibrational spectrum of the C-H stretching vibration of $\text{CH}^+\text{-He}$. upper part: PGOPHER simulation [37] displaying stick spectrum (black) and convoluted spectrum (red). lower part: experimental data of this work (green), including lines from previous work as given in Table 1 (blue sticks). The band origin of CH^+ at $2739.670097(5) \text{ cm}^{-1}$ [30], as well as the blue-shifted band origins of $\text{CH}^+\text{-He}$ and $\text{CH}^+\text{-He}_4$ (see Fig. 4) are indicated by dashed vertical lines. Branches of $\text{CH}^+\text{-He}$ are designated by the notation ${}^{\Delta K} \Delta J_K$.

constant $A_0 = 15.15 \text{ cm}^{-1}$ is determined by the tilt of the CH-unit towards this axis, i.e. by the Jacobi angle, for which we calculate $\theta_0 = 73.52^\circ$ for the ground vibrational state. Using also the rotational constant $B_0 = 1.0184 \text{ cm}^{-1}$ (see Table 2) we further estimate $R_0 = 2.319 \text{ \AA}$ (the distance between He and the center of mass of the CH subunit), in good agreement with the average value $R_0 = 2.4 \text{ \AA}$ given by Meuwly and Wright [27] for the ground vibrational state. In a similar way, using $r_1 = 1.162 \text{ \AA}$ for the vibrationally excited state probed in this work, we obtain an angle $\theta_1 = 74.79^\circ$ and a distance which is only slightly larger, $R_1 = 2.321 \text{ \AA}$.

4. Rovibrational spectroscopy of $\text{CH}^+\text{-He}_4$

In order to get more insight into the structure of the helium complexes, we also investigated $\text{CH}^+\text{-He}_4$ by IRPD. We chose this complex instead of $\text{CH}^+\text{-He}_2$ or $\text{CH}^+\text{-He}_3$, as the latter are suspected to be floppy with a complicated spectrum (and we postpone their investigation to a later work). $\text{CH}^+\text{-He}_4$, on the other hand, is predicted to be an oblate symmetric top [39], with a 4-membered ring of helium atoms surrounding the C-H axis. It thus belongs to the symmetry group C_{4v} . The IRPD spectrum of $\text{CH}^+\text{-He}_4$, measured by observing the mass channel $m = 29 \text{ u}$ (see Fig. 2) as a function of laser wavenumber, is shown in Fig. 4. It exhibits parallel transitions ($\Delta K = 0$) of a symmetric top molecule, thus confirming the proposed structure. At the resolution of this experiment, only the rotational constant B (the one perpendicular to the symmetry axis of the top) and the band origin can be determined with confidence, and are included in Table 2. As expected, the band origin, at $2763.77(5) \text{ cm}^{-1}$, is further blue shifted w.r.t. the ones of CH^+ and $\text{CH}^+\text{-He}$ (see also the dashed vertical lines in Fig. 3). As anticipated by theoretical work [39], these blue shifts seem very linear, and we obtain a value of about 6 cm^{-1} per additional He

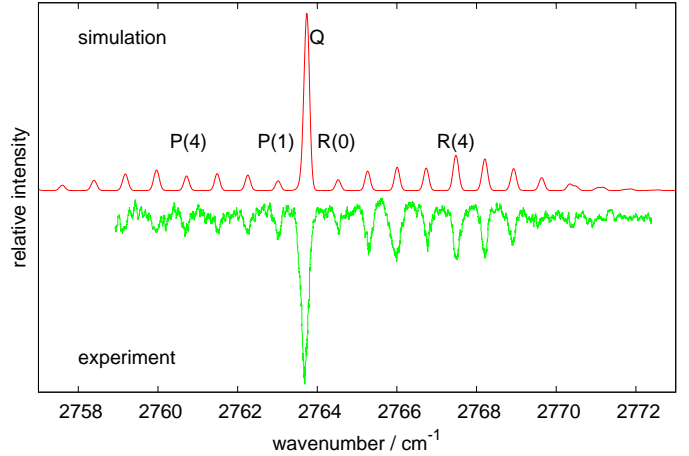


Figure 4: Rovibrational spectrum of the C-H stretching vibration of $\text{CH}^+\text{-He}_4$ (upper panel: PGOPHER simulation [37] in red, lower panel: experimental data in green). Some crosstalk of this spectrum into that of $\text{CH}^+\text{-He}$ can be observed in Fig. 3 (see e.g. the rightmost dashed vertical line in Fig. 3, which is the position of the Q-branch of $\text{CH}^+\text{-He}_4$). In the simulation, we took into account that only the nuclear spin weights of the irreducible representations A_1 and A_2 are non-zero.

atom. Therefore, we may predict band origins of 2751.7 cm^{-1} and 2757.7 cm^{-1} for the floppy $\text{CH}^+\text{-He}_2$ and $\text{CH}^+\text{-He}_3$, respectively.

The experimental rotational constant $B = 0.378 \text{ cm}^{-1}$ is in good agreement with the proposed structure of $\text{CH}^+\text{-He}_4$. Assuming this molecule to be formed by filling up the 4-membered ring with He atoms and having all a distance of about 2.22 \AA to the CH-axis as calculated for $\text{CH}^+\text{-He}$, we obtain a rotational constant $B = 0.384 \text{ cm}^{-1}$. This value even suggests that the distance of the He atoms to the CH-axis is slightly larger for $\text{CH}^+\text{-He}_4$ than for $\text{CH}^+\text{-He}$. In summary, this is consistent with the picture that in the $\text{CH}^+\text{-He}_n$ series, every additional He atom strengthens the C-H bond, leading to the mentioned additive blue shift of the band origin of about $6 \text{ cm}^{-1}/\text{He atom}$, while the $\text{CH}^+\text{-He}$ bonds get weaker, leading to slightly larger distances of the He atoms to the CH-axis.

5. Conclusions and Outlook

Using a combination of a cryogenic ion trap machine with a tunable table-top pulsed IR source the ν_1 C-H stretches of the cation-helium complexes $\text{CH}^+\text{-He}$ and $\text{CH}^+\text{-He}_4$ have been recorded in the $3 \mu\text{m}$ region. To the best of our knowledge, $\text{CH}^+\text{-He}_4$ is the largest cation-helium complex ($n = 4$) for which a rotationally resolved IR spectrum has been reported. The investigation confirms the proposed structures of $\text{CH}^+\text{-He}$ [27] and $\text{CH}^+\text{-He}_4$ [39], with the helium atoms attached to the C-H backbone in a T-shaped manner, by multiple evidence: i) the mass spectrum shows a magic number at 4 helium atoms and thus supports a 4-membered ring around the CH^+ axis, ii) the relatively long lifetime of the vibrationally excited $\text{CH}^+\text{-He}$ complex of about 1.6 ns is consistent with (but does not necessarily prove) the fact that the He-bond does not point along the C-H axis, iii) the band origins of the C-H stretch vibrations

Table 1: Rovibrational transitions of the ν_1 band of CH^+-He . Experimental uncertainties are given in parentheses.

| | $J'_{Ka'Kc'} \leftarrow J''_{Ka''Kc''}$ | $\tilde{\nu} / \text{cm}^{-1}$ | Obs.-Calc. | τ / ns^a |
|--------------|---|--------------------------------|------------|----------------------|
| ${}^pP_1(3)$ | $2_{02} \leftarrow 3_{13}$ | 2726.14(5) | 0.015 | |
| ${}^pP_1(2)$ | $1_{01} \leftarrow 2_{11}$ | 2727.97(5) | -0.003 | |
| ${}^pP_1(1)$ | $0_{00} \leftarrow 1_{11}$ | 2729.86(5) | 0.002 | |
| pQ_1 | | 2731.7 | | |
| ${}^pR_1(1)$ | $2_{02} \leftarrow 1_{11}$ | 2735.69(5) | 0.012 | |
| ${}^pR_1(2)$ | $3_{03} \leftarrow 2_{12}$ | 2737.67(5) | 0.010 | |
| ${}^pR_1(3)$ | $4_{04} \leftarrow 3_{13}$ | 2739.63(5) | -0.031 | |
| ${}^rP_0(4)$ | $3_{13} \leftarrow 4_{04}$ | 2751.32(5) | 0.027 | |
| ${}^rP_0(3)$ | $2_{12} \leftarrow 3_{03}$ | 2753.40(5) | 0.015 | |
| ${}^rP_0(2)$ | $1_{11} \leftarrow 2_{02}$ | 2755.46(5) | 0.019 | |
| rQ_0 | | 2759.45 | | |
| ${}^rR_0(0)$ | $1_{11} \leftarrow 0_{00}$ | 2761.27(5) | -0.034 | |
| ${}^rR_0(1)$ | $2_{12} \leftarrow 1_{01}$ | 2763.13(5) | -0.005 | |
| ${}^rR_0(2)$ | $3_{13} \leftarrow 2_{02}$ | 2764.92(5) | 0.018 | |
| ${}^rR_0(3)$ | $4_{14} \leftarrow 3_{03}$ | 2766.607175(8) ^{b,c} | 0.0 | 1.50(2) |
| ${}^rR_0(4)$ | $5_{15} \leftarrow 4_{04}$ | 2768.254(1) ^b | 0.0 | 1.63(7) |
| ${}^rQ_1(3)$ | $3_{21} \leftarrow 3_{12}$ | 2785.315(1) ^b | 0.0 | 1.4(2) |
| ${}^rQ_1(2)$ | $2_{20} \leftarrow 2_{11}$ | 2785.468(1) ^b | 0.0 | 1.5(1) |
| ${}^rQ_1(3)$ | $3_{22} \leftarrow 3_{13}$ | 2785.791(1) ^b | 0.0 | 1.8(5) |
| ${}^rR_1(1)$ | $2_{20} \leftarrow 1_{11}$ | 2789.534(1) ^b | 0.0 | 1.61(6) |
| ${}^rR_1(2)$ | $3_{21} \leftarrow 2_{11}$ | 2791.51941(2) ^{b,c} | 0.0 | 1.65(3) |

^a The lifetimes are determined by extracting the Lorentzian width in a Voigt fit, assuming the Gaussian contribution to correspond to a temperature of 14 K

^b The seven CH^+-He lines with higher precision have been detected in our previous work [30].

^c lines with very high precision and accuracy have been measured with a frequency comb system.

of CH^+-He and CH^+-He_4 , when compared to the one of CH^+ (2739.670097(5) cm^{-1} [30]), exhibit blue shifts which are quite small and show a regular additive behavior, and finally, iv) the full spectral analyses given in the preceding sections reveals CH^+-He and CH^+-He_4 to have rotational constants which are in close agreement with the proposed structures. It is astonishing that such potentially floppy molecules with weak bonds of the helium atoms to the CH^+ core present themselves as textbook-like rigid near-prolate and oblate symmetric tops, respectively, at least at the resolution of the current experiment. Further high-resolution experiments are necessary to reveal deviations from a perfect rigid rotor model and to explore the shallow potential energy surface via the determination of the higher order centrifugal distortion constants.

The CH^+-He complex can be compared to other complexes which have a linear cation core. Typically, complexes of the type AH^+-He (with AH^+ being the linear cation core) exhibit a linear proton-bound structure, leading to a redshift of the A-H vibrational frequency upon complexation with He, as witnessed for the mentioned systems HCO^+-He [7, 8], OH^+-He [9], $\text{N}_2\text{H}^+-\text{He}$ [6], HeH^+-He [18], and H_2^+-He [40]. To the best of our knowledge, CH^+-He is the only such complex with a T-shaped structure. CH^+-He and CH^+-He_4 are thus somewhat more similar to the H^+-He_n series of complexes, for which the symmetric linear complex with $n = 2$, $\text{He}-\text{H}^+-\text{He}$, has been determined as the central core, and with $n = 3$ having a T-

shaped structure and $n = 6$ a 4-membered helium ring around this core. While low-resolution IR studies could confirm these motifs [17], high-resolution studies for $n \geq 3$ are currently hampered by lifetime broadening [18].

More detailed information about the structure of CH^+-He can also be obtained by the investigation of its ground vibrational state. Rotational spectroscopy of CH^+-He is feasible as it possess a permanent dipole moments along both the a- and b-axes (see Fig. 1). We expect the dipole moment along the a-direction to be particularly strong, as the charge sits mainly on the CH^+ moiety which is separated by more than 2 Å from the He atom. A rough prediction of the a-type and b-type rotational spectra can be found in Fig. 5. High-resolution rotational spectroscopy of CH^+-He can be achieved by combining the IRPD spectroscopy presented in this work with a rotational photon in a double-resonance scheme, as recently demonstrated for the complexes CH_3^+-He and HCO^+-He [11, 8]. As shown in those works, the rotational spectroscopy of loosely bound complexes is not limited by lifetime and broadening issues, so that accurate quantum state information on the kHz-level can be obtained.

Acknowledgements

This work has been supported via Collaborative Research Centre 956, sub-project B2, funded by the Deutsche Forschungsgemeinschaft (DFG, project ID 184018867) as well

Table 2: Spectroscopic parameters for $\text{CH}^+\text{-He}$ and $\text{CH}^+\text{-He}_4$. All values in cm^{-1} . Experimental uncertainties are given in parentheses. Spectroscopic fits were done with the program PGOPHER [37].

| | ab initio ^a | | this work | |
|-----------------------------------|------------------------|-------------------|------------|-------------|
| | ground | $\nu_1 = 1$ | ground | $\nu_1 = 1$ |
| $\text{CH}^+\text{-He}, C_s$ | | | | |
| ν | | 2869 ^b | | 2745.94(1) |
| A | 15.28 | | 15.15(1) | 14.435(2) |
| \bar{B} | 0.93 | | 0.9785(2) | 0.9708(4) |
| $B - C$ | 0.074 | | 0.07972(9) | 0.091(3) |
| $D_J \times 10^3$ | | | 0.23(1) | 0.13(2) |
| $\text{CH}^+\text{-He}_4, C_{4v}$ | | | | |
| ν | | | | 2763.77(5) |
| B | | | 0.378(1) | 0.375(1) |

^a Reference [27]

^b harmonic value

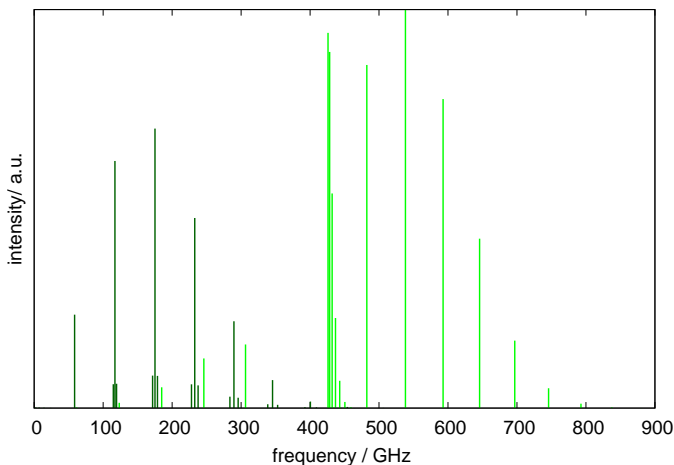


Figure 5: Prediction of the expected rotational spectrum of $\text{CH}^+\text{-He}$ at $T = 10$ K, based on the spectroscopic parameters given in Table 2. The a-type ($\Delta K_a = 0, \Delta K_c = \pm 1$) and the b-type ($\Delta K_a = \pm 1, \Delta K_c = \pm 1$) transitions are shown in dark green and light green, respectively.

as DFG SCHL 341/15-1 (“Cologne Center for Terahertz Spectroscopy”) and AS 319/2-2. JLD acknowledges partial financial support from the Agencia Estatal de Investigación (AEI) through grant FIS2016-77726-C3-1-P and from the European Research Council through grant agreement ERC-2013-SyG-610256-NANOCOSMOS. We thank the anonymous reviewer for a thorough check of the submitted manuscript.

References

- [1] D. W. Boo, Z. Liu, A. G. Suits, J. Tse, Y. T. Lee, Dynamics of Carbonium Ions Solvated by Molecular Hydrogen: $\text{CH}_5^+(\text{H}_2)_n$ ($n=1,2,3$), *Science* 269 (1995) 57–59.
- [2] E. Bieske, O. Dopfer, High resolution spectroscopy of ionic complexes, *Chem. Rev.* 100 (2000) 3963–3998.
- [3] M. Brümmer, C. Kaposta, G. Santambrogio, K. R. Asmis, Formation and photodepletion of cluster ion–messenger atom complexes in a cold ion trap: Infrared spectroscopy of VO^+ , VO_2^+ , and VO_3^+ , *J. Chem. Phys.* 119 (24) (2003) 12700–12703.
- [4] J. Jašík, J. Žabka, J. Roithová, D. Gerlich, Infrared spectroscopy of trapped molecular dications below 4 K, *Int. J. Mass Spectrom.* 354 (2013) 204–210.
- [5] J. Jašík, R. Navrátil, I. Němec, J. Roithová, Infrared and Visible Photodissociation Spectra of Rhodamine Ions at 3 K in the Gas Phase, *J. Phys. Chem. A* 119 (51) (2015) 12648–12655.
- [6] S. A. Nizkorodov, J. P. Maier, E. J. Bieske, The infrared spectrum of the $\text{N}_2\text{H}^+\text{-He}$ ion-neutral complex, *J. Chem. Phys.* 102 (13) (1995) 5570–5571.
- [7] S. A. Nizkorodov, J. P. Maier, E. J. Bieske, The infrared spectrum of He-HCO^+ , *J. Chem. Phys.* 103 (4) (1995) 1297–1302.
- [8] T. Salomon, M. Töpfer, P. Schreier, S. Schlemmer, H. Kohguchi, L. Surin, O. Asvany, Double resonance rotational spectroscopy of He-HCO^+ , *Phys. Chem. Chem. Phys.* 21 (2019) 3440–3445.
- [9] D. Roth, S. A. Nizkorodov, J. P. Maier, O. Dopfer, Intermolecular interaction in the $\text{OH}^+\text{-He}$ and $\text{OH}^+\text{-Ne}$ open-shell ionic complexes: Infrared predissociation spectra of the ν_1 and $\nu_1 + \nu_b$ vibrations, *J. Chem. Phys.* 109 (10) (1998) 3841–3849.
- [10] R. V. Olkhov, S. A. Nizkorodov, O. Dopfer, Intermolecular interaction in the $\text{CH}_3^+\text{-He}$ ionic complex revealed by ab initio calculations and infrared photodissociation spectroscopy, *J. Chem. Phys.* 110 (1999) 9527–9535.
- [11] M. Töpfer, T. Salomon, S. Schlemmer, O. Dopfer, H. Kohguchi, K. M. T. Yamada, O. Asvany, Double resonance rotational spectroscopy of weakly bound ionic complexes: the case of floppy $\text{CH}_3^+\text{-He}$, *Phys. Rev. Lett.* 121 (2018) 143001.
- [12] E. Bieske, A. Soliva, A. Friedmann, J. Maier, Vibrational predissociation lifetime of $\text{N}_2^+\text{-He}$ ($X, \nu = 1$), *J. Chem. Phys.* 96 (5) (1992) 4035–4036.
- [13] N. Lakin, R. Olkhov, O. Dopfer, Internal rotation in $\text{NH}_4^+\text{-Rg}$ dimers (Rg = He, Ne, Ar): Potential energy surfaces and IR spectra of the ν_3 band, *Faraday Discuss.* 118 (2001) 455–76; discussion 487.
- [14] S. A. Nizkorodov, D. Roth, R. V. Olkhov, J. P. Maier, O. Dopfer, Infrared predissociation spectra of He-HO_2^+ and Ne-HO_2^+ : prediction of the ν_1 frequency of HO_2^+ , *Chem. Phys. Lett.* 278 (1) (1997) 26–30.
- [15] H. Kohguchi, P. Jusko, K. M. T. Yamada, S. Schlemmer, O. Asvany, High-resolution infrared spectroscopy of O_2H^+ in a cryogenic ion trap, *J. Chem. Phys.* 148 (2018) 144303.
- [16] I. Savić, D. Gerlich, O. Asvany, P. Jusko, S. Schlemmer, Controlled synthesis and analysis of He-H_3^+ in a 3.7 K ion trap, *Mol. Phys.* 113 (15-16) (2015) 2320–2332.
- [17] O. Asvany, S. Schlemmer, T. Szidarovszky, A. G. Császár, Infrared signatures of the HHe_n^+ and DHe_n^+ ($n = 3 - 6$) complexes, *J. Phys. Chem. Lett.* 10 (2019) 5325–5330.
- [18] M. Töpfer, A. Jensen, K. Nagamori, H. Kohguchi, T. Szidarovszky, A. G. Császár, S. Schlemmer, O. Asvany, Spectroscopic signatures of HHe_2^+ and HHe_3^+ , *Phys. Chem. Chem. Phys.* 22 (2020) 22885–22888.
- [19] T. Dunham, Interstellar Neutral Potassium and Neutral Calcium, *Publ. Astron. Soc. Pacific* 49 (1937) 26.
- [20] A. E. Douglas, G. Herzberg, Note on CH^+ in Interstellar Space and in the Laboratory, *Astrophys. J.* 94 (1941) 381.
- [21] J. Cernicharo, X.-W. Liu, E. González-Alfonso, P. Cox, M. J. Barlow, T. Lim, B. M. Swinyard, Discovery of Far-Infrared Pure Rotational Transitions of CH^+ in NGC 7027, *Astrophys. J.* 483 (1997) L65–L68.
- [22] E. Falgarone, T. Phillios, J. C. Pearson, First detection of $^{13}\text{CH}^+$ ($J = 1 - 0$), *Astrophys. J. Lett.* 634 (2005) L149–L152.
- [23] K. M. Menten, F. Wyrowski, A. Belloche, R. Güsten, L. Dedes, H. S. P. Müller, Submillimeter absorption from SH^+ , a new widespread interstellar radical, $^{13}\text{CH}^+$ and HCl , *Astron. Astrophys.* 525 (2011) A77.
- [24] Z. Nagy, F. F. S. Van der Tak, V. Ossenkopf, M. Gerin, F. Le Petit, J. Le Bourlot, J. H. Black, J. R. Goicoechea, C. Joblin, M. Röllig, E. A. Bergin, The chemistry of ions in the Orion Bar I. – CH^+ , SH^+ , and CF^+ , *Astron. Astrophys.* 550 (2013) A96.
- [25] D. A. Neufeld, M. Goto, T. R. Geballe, R. Güsten, K. M. Menten, H. Wiesemeyer, Detection of Vibrational Emissions from the Helium Hydride Ion (HeH^+) in the planetary nebula NGC 7027, *Astrophys. J.* 894 (2020) 37.
- [26] J. M. Hughes, E. I. von Nagy-Felsobuki, Ab initio investigations of the electronic structure of HeCH^+ and HeCH_2^+ , *Chem. Phys. Lett.* 272 (5) (1997) 313–318.
- [27] M. Meuwly, N. J. Wright, The Potential Energy Surface and Rotational-Vibrational States of He-CH^+ , *J. Phys. Chem. A* 104 (6) (2000) 1271–1277.

- [28] T. Stoecklin, A. Voronin, Vibrational and rotational energy transfer of CH^+ in collisions with ^4He and ^3He , *Eur. Phys. J. D* 46 (2008) 259 – 265.
- [29] K. Hammami, L. Owono Owono, N. Jaidane, Z. Ben Lakhdar, Rotational excitation of methylidyne (CH^+) by helium atom at low temperature, *Journal of Molecular Structure: THEOCHEM* 853 (1) (2008) 18 – 26.
- [30] J. L. Doménech, P. Jusko, S. Schlemmer, O. Asvany, The first laboratory detection of vibration-rotation transitions of $^{12}\text{CH}^+$ and $^{13}\text{CH}^+$ and improved measurement of their rotational transition frequencies, *Astrophys. J.* 857 (2018) 61.
- [31] O. Asvany, S. Brünken, L. Kluge, S. Schlemmer, COLTRAP: a 22-pole ion trapping machine for spectroscopy at 4 K, *Appl. Phys. B* 114 (2014) 203–211.
- [32] S. Thorwirth, P. Schreier, T. Salomon, S. Schlemmer, O. Asvany, Pure rotational spectrum of CN^+ , *Astrophys. J.* 882 (2019) L6.
- [33] O. Asvany, F. Biela, D. Moratschke, J. Krause, S. Schlemmer, New design of a cryogenic linear RF multipole trap, *Rev. Sci. Instr.* 81 (2010) 076102.
- [34] S. Brünken, L. Kluge, A. Stoffels, J. Pérez-Ríos, S. Schlemmer, Rotational state-dependent attachment of He atoms to cold molecular ions: An action spectroscopic scheme for rotational spectroscopy, *J. Mol. Spectros.* 332 (2017) 67 – 78.
- [35] O. Asvany, H. Krüger, S. Schlemmer, Simple o-ring sealed Brewster-angle window for ultrahigh vacuum applications, *Journal of Vacuum Science & Technology B* 38 (4) (2020) 045001.
- [36] O. Asvany, J. Krieg, S. Schlemmer, Frequency comb assisted mid-infrared spectroscopy of cold molecular ions, *Rev. Sci. Instr.* 83 (2012) 093110.
- [37] C. M. Western, Pgoopher: A program for simulating rotational, vibrational and electronic spectra, *J. Quant. Spectros. Rad. Transfer* 186 (2017) 221 – 242.
- [38] T. Amano, The $J = 1-0$ Transitions of $^{12}\text{CH}^+$, $^{13}\text{CH}^+$, and $^{12}\text{CD}^+$, *Astrophys. J. Lett.* 716 (2010) L1–L3.
- [39] M. Solimannejad, B. S. Mirhoseini, M. D. Esrafil, Microsolvation of CH^+ in helium: An ab initio study, *J. of Theoretical and Comp. Chem.* 15 (2016) 1650018.
- [40] D. Koner, J. C. San Vicente Veliz, A. van der Avoird, M. Meuwly, Near dissociation states for $\text{H}_2^+ - \text{He}$ on MRCI and FCI potential energy surfaces, *Phys. Chem. Chem. Phys.* 21 (2019) 24976–24983.